Difference structures from time-resolved small-angle and wide-angle x-ray scattering

Prakash Nepal* and D. K. Saldin
Department of Physics, University of Wisconsin–Milwaukee, P.O. Box 413, Milwaukee, Wisconsin 53201, USA

(Received 14 October 2016; revised manuscript received 27 April 2018; published 17 May 2018)

Time-resolved small-angle x-ray scattering/wide-angle x-ray scattering (SAXS/WAXS) is capable of recovering difference structures directly from difference SAXS/WAXS curves. It does so by means of the theory described here because the structural changes in pump-probe detection in a typical time-resolved experiment are generally small enough to be confined to a single residue or group in close proximity which is identified by a method akin to the difference Fourier method of time-resolved crystallography. If it is assumed, as is usual with time-resolved structures, that the moved atoms lie within the residue, the 100-fold reduction in the search space (assuming a typical protein has about 100 residues) allows the exaction of the structure by a simulated annealing algorithm with a huge reduction in computing time and leads to a greater resolution by varying the positions of atoms only within that residue. This reduction in the number of potential moved atoms allows us to identify the actual motions of the individual atoms. In the case of a crystal, time-resolved calculations are normally performed using the difference Fourier method, which is, of course, not directly applicable to SAXS/WAXS. The method developed in this paper may be thought of as a substitute for that method which allows SAXS/WAXS (and hence disordered molecules) to also be used for time-resolved structural work.

DOI: 10.1103/PhysRevB.97.195426

I. INTRODUCTION

Due to the fact that the amount of data from small-angle x-ray scattering/wide-angle x-ray scattering (SAXS/WAXS) is confined to a single $I(q)$ curve (where q is a scalar) it is generally believed that SAXS/WAXS spectra are good only for obtaining a relatively low resolution envelope of the molecule. Nevertheless, as has been shown by Stuhrmann [1,2] and Svergun and Stuhrmann [3] there is enough information in an experimental SAXS spectrum to obtain at least a low-resolution structure of the molecule being studied. This is based on the assumption that the width of a peak in SAXS is approximately the size of a Shannon pixel π/L, where L is the width of the molecule. Given the width of a typical SAXS curve, this normally translates to about 20 pieces of information, enough for the extraction of the spherical harmonic expansion coefficients up to an angular momentum quantum number of perhaps $l = 3$ for the electron density of the molecule, which gives a low-resolution structure and nothing more. It is true that at higher q's the results from experiment are dominated by Poisson noise. However, Poisson noise is not a serious impediment, as it is known that many averages of Poisson noise give rise to the expected result. The procedure of averaging has been exploited in many fields before. For example, bare electron microscopy (EM) images in cryo-EM hardly show anything useful, yet after much averaging a clear picture of a biomolecule emerges. In fact, all that is needed is the measurement of a large number of noisy diffraction patterns from which the SAXS/WAXS can be extracted. There is also an extra piece of information in time-resolved SAXS/WAXS that has not been exploited much before, namely, knowledge of the unperturbed structure. We show in this paper that one can use this extra information to help find details about the inside of a molecule from time-resolved SAXS/WAXS.

Time-resolved protein crystallography [4] is based on the difference Fourier approximation in which the phases of a perturbed (p) state are approximated by the phases of a similar unperturbed (u) structure. Since the amplitudes of the perturbed structure are found from experiment, this enables the difference electron density to be found using Fourier transformation and hence the time variation of a structure. The difference Fourier method is not applicable to SAXS/WAXS as the basic experimental data consist of the incoherent averages of intensities over all directions. Nevertheless, as we show in this paper, it is possible to derive a method to find the difference structure directly from SAXS/WAXS data. The best that can be hoped for from a "direct" method of solution is a structure in which the number of real-space points is about equal to the number of data points. Given the limited amount of information in a SAXS curve, the best that can be hoped for with a direct method is a low-resolution structure. However, even a low-resolution structure can act as a springboard for much higher resolution if it is known that the atoms whose positions need to be varied in a standard fitting scheme lie in the vicinity of the peaks in the initial low-resolution map. Given that current global optimization routines can be regarded more as refinement methods than *ab initio* structure determination methods, even an indication of where the structure lies can be a great help in determining an accurate structure with model fitting. In step 1 of our method, we illustrate the identification of the moved residues with an application to photoactive yellow protein, which is often used as a test case in time-resolved crystallography [5]. We subsequently describe using this information to find the internal structure of photoactive yellow protein (PYP).

Although they are quite easy to arrange in crystallography, equal numbers of data points and points at which one seeks the

*Corresponding author: pnepal@uwm.edu

electron density are much more difficult in SAXS/WAXS due to the paucity of the data. It is reasonable to question whether the crystals themselves give rise to a kind of steric hindrance that may make the time-resolved changes be not exactly the same as what is found in nature. Of course, it is arguable that molecules in nature form a kind of "crowded" environment whose density is closer to a crystalline state than the dilute ensemble usually studied using SAXS/WAXS. Nevertheless, they certainly do not form the ordered arrangement of a crystal. The outcome is completely determined when the matrices relating the data to the number of points in real space are known.

II. THE RAPID DIRECT METHOD

The starting point in our theory is the relation between a SAXS/WAXS spectrum and a scattering amplitude of the molecule that is familiar in crystallography. In general a scattering amplitude $F_{u,p}(\mathbf{q})$ of unperturbed and perturbed structures, respectively, may be written in terms of their respective electron densities $\rho_{u,p}(\mathbf{r})$. By treating the problem as one of finding a perturbed structure from the knowledge of an unperturbed structure one encompasses proposed mix-and-inject experiments [6] as well as ones based on photoexcitation [4,7].

$$F_{u,p}(\mathbf{q}) = \int \rho_{u,p}(\mathbf{r}) \exp(i\mathbf{q}\cdot\mathbf{r}) d\mathbf{r}. \tag{1}$$

An alternative way of calculating such a scattering amplitude is from the data in the Protein Data Bank (PDB) [8] file via

$$F_{u,p}(\mathbf{q}) = \sum_n f_n \exp(i\mathbf{q}\cdot\mathbf{r}_n). \tag{2}$$

The SAXS/WAXS intensity expected from such an experiment is

$$I_{u,p}(q) = \int |F_{u,p}(\mathbf{q})|^2 d\hat{\mathbf{q}} = \int F^* u, p(\mathbf{q}) F_{u,p}(\mathbf{q}) d\hat{\mathbf{q}}. \tag{3}$$

Consequently, measured quantities in a SAXS/WAXS experiment are not only related to the square moduli of the scattering amplitudes, as in x-ray crystallography, but also related to an angular integral of the square moduli. When added to the paucity of data from experiment, it is not surprising that the theory of the extraction of electron density directly from the SAXS/WAXS data is very difficult. Nevertheless, as we show here, it is not impossible through a combination of the ideas we describe. First, we think of the quantities that we want to relate, the difference SAXS/WAXS intensity and the difference electron density. We remember that we are considering a difference experiment where both the difference in the intensity and the difference in the electron density are very small. Perhaps a relationship exists in this limit. And, indeed, one does. First take the variation of (3). This gives the equation

$$\delta I_u(q) = \int \{\delta F_u^*(\mathbf{q}) F_u(\mathbf{q}) + F_u^*(\mathbf{q}) \delta F_u(\mathbf{q})\} d\hat{\mathbf{q}}. \tag{4}$$

The crucial steps are now identifying $\delta I_u(q)$ with the experimentally determined difference SAXS/WAXS spectrum

$$I_p(q) - I_u(q) \tag{5}$$

and a relation of $\delta F_u(\mathbf{q})$ to a difference electron density. The latter may be found by just taking the variation of (1). The functional differentiation is performed with respect to just electron density $\rho(\mathbf{r})$ [9]. This gives

$$\delta F_u(\mathbf{q}) = \int \delta\rho_u(\mathbf{r}) \exp(i\mathbf{q}\cdot\mathbf{r}) d\mathbf{r} \tag{6}$$

Moreover, by exploiting the smallness of these quantities in a time-resolved experiment, it is possible to show that the relationship is linear in the limit of small changes. This means it is possible to find an invertible matrix relation between the two where the elements of the matrix are constant. With modern matrix inversion techniques, it is possible to invert a linear matrix equation even if the amount of data from experiment does not match the number of points at which the difference density is sought.

The sum over n here is over all atoms in the structure. Now we give some technical details. The angular integral in (4) is best done using the orthogonality relation

$$\int Y_{lm}^*(\hat{\mathbf{q}}) Y_{l'm'}(\hat{\mathbf{q}}) d\hat{\mathbf{q}} = \delta_{ll'}\delta_{mm'} \tag{7}$$

in spherical coordinates. This is most easily done by substituting the spherical expansion of a plane wave, namely,

$$\exp(i\mathbf{q}\cdot\mathbf{r}_n) = 4\pi \sum_{lm} i^l j_l(qr_n) Y_{lm}(\hat{\mathbf{q}}) Y_{lm}^*(\hat{\mathbf{r}}_n), \tag{8}$$

in (1). Then we use the spherical expansion of the scattering amplitudes,

$$F_{u,p}(\mathbf{q}) = \sum_{lm} F_{lm}^{(u,p)}(q) Y_{lm}(\hat{\mathbf{q}}), \tag{9}$$

and find from (2)

$$F_{lm}^{(u,p)}(q) = 4\pi \sum_n i^l f_n j_l(qr_n) Y_{lm}^*(\hat{\mathbf{r}}_n). \tag{10}$$

In the last expression the sum over n is a sum over atoms in a PDB file, and this is actually a very convenient way to calculate the SAXS/WAXS spectra via

$$I_{u,p}(q) = \sum_{lm} \left|F_{lm}^{(u,p)}(q)\right|^2, \tag{11}$$

with the angular average done analytically. Note that we calculate both $I_u(q)$ and $I_p(q)$ only for the test in this paper. In practice, $I_p(q)$ is found from experiment, and only $I_u(q)$ needs to be calculated. We take the SAXS/WAXS intensities in their spherical representation, where the angular average has already been performed.

In a time-resolved experiment one measures multiple diffraction patterns in quick succession. A particular structure is assumed to not change by very much in such a short time interval. It is hoped that a comparison of the diffraction patterns will reveal the time variation of the structure. In time-resolved crystallography this is provided by the difference Fourier method. We investigate here whether similar information can be obtained from a time-resolved SAXS/WAXS experiment. For our test purposes the SAXS intensities $I_u(q)$ and $I_p(q)$ are both calculated from Eqs. (2), (10), and (11). In a practical application, of course, I_p comes from experiment and does not need to be calculated. It is only necessary to calculate I_u from knowledge of the "dark" structure.

Representing the intensities and scattering amplitudes in spherical coordinates allows the necessity of angular averages for SAXS/WAXS to be carried out. Substituting (2) and (6) into (4), we may deduce the relationship between the difference SAXS/WAXS spectrum and the difference electron density sought, namely,

$$\delta I_u(q) = \sum_k M_{q,\mathbf{k}} \delta\rho_u(\mathbf{r_k}), \tag{12}$$

where $\mathbf{r_k}$ are taken to be a uniform set of Cartesian grid points at which the electron density of the molecule is required. It is what exactly constitutes small is best investigated by the kind of modeling we do here. Simulations like this suggest that the approximation is valid for most small structural changes in PYP that accompany photoexcitation. The elements of the matrix in (12) are of the form

$$M_{q,\mathbf{k}} = \int \sum_k \{F_u(\mathbf{q}) \exp(-i\mathbf{q}.\mathbf{r}_k) + \text{c.c.}\} d\hat{\mathbf{q}}, \tag{13}$$

where c.c. refers to the complex conjugate. The angular integral is best done using (7). We then obtain

$$M_{q,\mathbf{k}} = 4\pi \sum_{lm} j_l(qr_k)\left\{i^{-l} F_{lm}^{(u)}(q) Y_{lm}(\hat{\mathbf{r}}_k) + \text{c.c.}\right\}. \tag{14}$$

As for the spherical harmonic expansion coefficients F_{lm} of the scattering amplitude F, they may be calculated from the data in the PDB file using expression (10). In the expressions for F_u (F_p) the sums are over the atoms in the relevant PDB files, and j_l is a spherical Bessel function of order l. Inverting Eq. (12), we obtain the relationship we seek, namely,

$$\delta\rho_u(\mathbf{r}_k) = M^{-1}_{\mathbf{k},q} \delta I_u(q), \tag{15}$$

which calculates an approximate difference density $\delta\rho_u(\mathbf{r}_k)$ at positions $\mathbf{r}_k$ of the difference SAXS spectrum $\delta I_u(q)$ by multiplication by the elements $(M^{-1})_{\mathbf{k},q}$ of the inverse of the matrix M.

III. MATRIX INVERSION WITH SINGULAR-VALUE DECOMPOSITION

The singular-value decomposition (SVD) of a real matrix M (M is an $m \times n$ matrix where $m > n$) is the product of three decomposed matrices. $M = USV^t$, where U is an $m \times m$ matrix, S is an $m \times n$ matrix, and V is an $n \times n$ matrix. V and U have the orthogonal property that

$$V^t V = I, \tag{16}$$

$$U^t U = I, \tag{17}$$

and S has only diagonal elements. The elements are in decreasing order and non-negative such that

$$s_1 \geqslant s_2 \geqslant s_3 \cdots \geqslant s_n \geqslant 0. \tag{18}$$

The condition number of M is the ratio $\frac{s_1}{s_n}$. The truncated SVD is used to compute matrix inversion to solve for $\delta\rho$. Then the system of equations becomes

$$\delta I_u = M \delta\rho_u, \tag{19}$$

which is represented as

$$\delta\rho_u = \sum_{i=1}^{n' \leqslant n} \frac{u_i^t \delta I_u}{s_i} v_i. \tag{20}$$

The columns matrices of V and U are, respectively, represented as v_i and u_i. The smaller singular values do not decay as

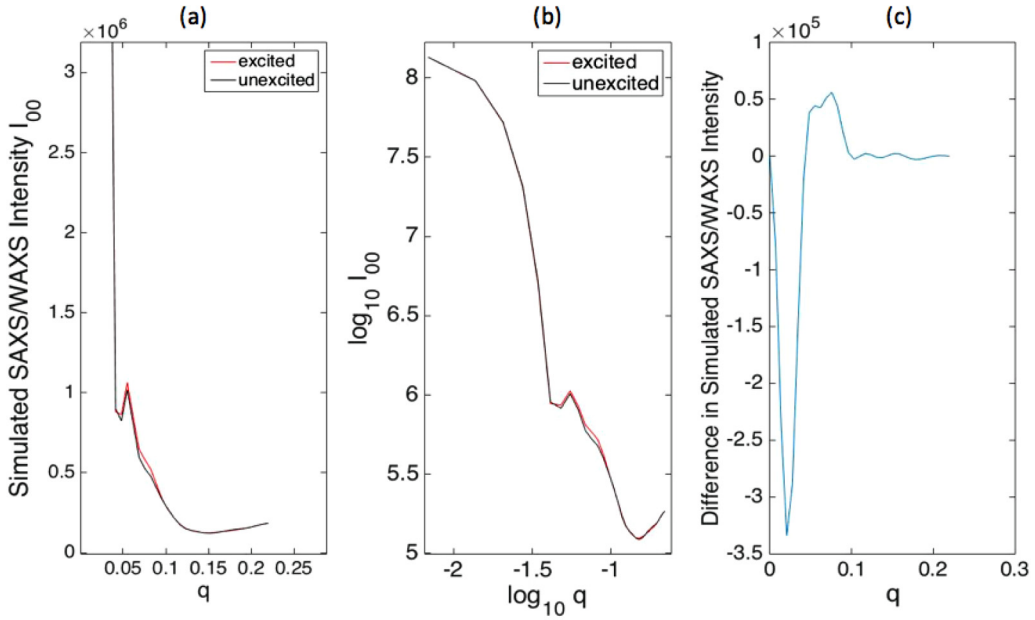

FIG. 1. (a) Theoretical (simulated) SAXS/WAXS intensities for unexcited and excited PYP structures with chromophore swing. Note that the red plot seems almost superimposed on the black one below $q = 0.05$; however, there is some difference between the two, as noted on the difference intensities curve. (b) Double-logarithmic plot of simulated SAXS/WAXS intensities for unexcited and excited PYP structures with chromophore swing. (c) Difference in theoretical SAXS/WAXS intensity for the chromophore swing case. The q values are in crystallographic convention (units: Å^{-1}).

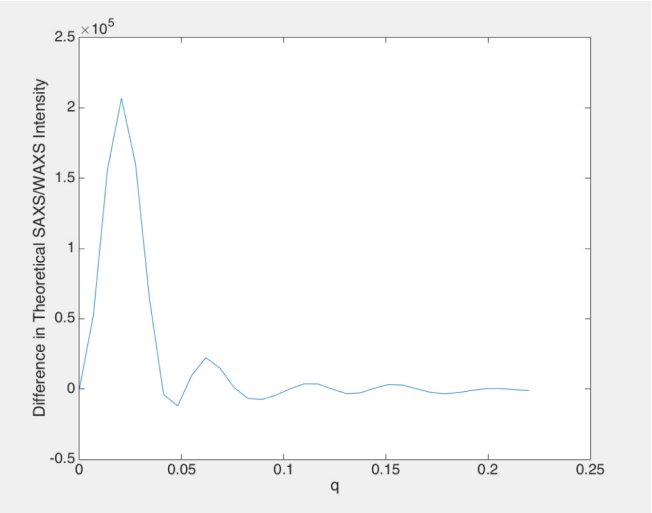

FIG. 2. Difference in theoretical (simulated) SAXS/WAXS intensity for ARG 124 Change. The q values are in crystallographic convention (units: Å^{-1}).

fast as the initial bigger singular values but tend to level off, and the solution is dominated by the terms in the sum corresponding to the smallest s_i [10]. Therefore, the truncation is necessary.

IV. OUTPUT OF THE RAPID DIRECT METHOD

Difference in simulated SAXS/WAXS intensities for unexcited and excited PYP structures with chromophore swing are shown in Fig. 1(c) and for Arginine 124 change is in Fig. 2. The output of the rapid direct method is shown in Figs. 3 and 5 for photoactive yellow protein.

Note that if we use the information present in the peaks and dips of the electron density, those peaks and dips correctly identify the residues containing the moved atoms, although not much more due to the limitations of SAXS/WAXS data. However, it correctly identifies the residue in which the atomic displacements occur. It is clear following a comparison with Figs. 3 and 4, on the one hand, and Figs. 5 and 6, on the other hand, that due to the paucity of data in SAXS/WAXS we cannot reconstruct an image of too high a resolution from only step 1 of our algorithm. In order to overcome this limitation we then embarked on step 2, which uses a simulated annealing method. Such a method is notorious in its bad scaling with the number of parameters varied. This is where we use the fact that the low-resolution maps recovered from step 1 of our algorithm, although low resolution, are nevertheless able to recover the residue in which the atoms that are displaced are found.

In step 2 we exploit this fact to reduce the number of displaced atoms whose positions need to be searched for by our simulated annealing algorithm.

V. SIMULATED ANNEALING

Even if we can obtain only a resolution to the level of identifying the residue in which atoms have changed their positions, since the average residue in a protein has only a relatively small number of atoms, we expect it will not be too difficult to vary only the positions of these atoms with

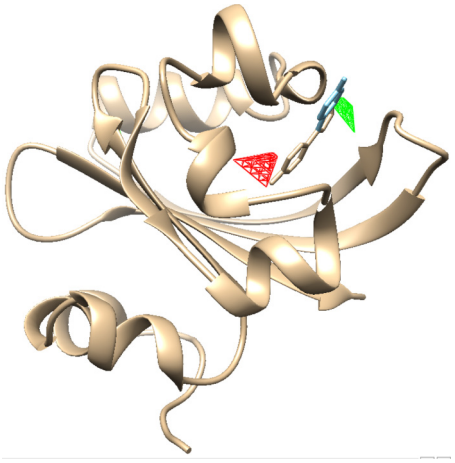

FIG. 3. Electron density differences between the photoexcited PYP [11] assumed and the "dark" structure of PYP (PDB ID 2phy) [12] from step 1 of our algorithm. Note that in this step we use only the highest and lowest values of the density differences, so the contour level is chosen to show only these. Consistent with the convention in time-resolved crystallography, the positive difference electron density (towards which the chromophore moves) is indicated by the green lobe, and the negative electron density (from which the chromophore has moved) is indicated by the red one. The value for $q_{\max}$ is 0.22 Å^{-1} (crystallographic), corresponding to a resolution of about 5 Å, with maps calculated for a $50 \times 50 \times 50$ Å^3 box with an $11 \times 11 \times 11$ grid. This figure was produced with CHIMERA [16].

a global optimization algorithm such as simulated annealing [13] to get a reasonably accurate solution [14]. In other words we perform the first step only to narrow down the simulated annealing search. This is essential with a method such as simulated annealing which scales in a disadvantageous way with the number of atoms N whose positions are sought (in fact, Rous [15] finds evidence that the time for a calculation may vary as N^6).

The method of simulated annealing has become established as a method of global optimization in which one varies the values of certain parameters on which a spectrum depends according to a general protocol until one obtains the parameters

FIG. 4. Same as Fig. 7, except using the difference Fourier method of classical time-resolved crystallography.

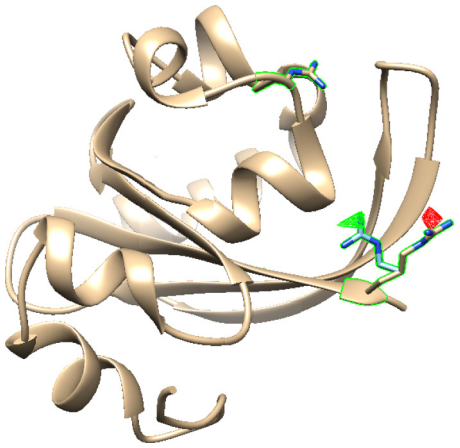

FIG. 5. Same as Fig. 3, except that the same difference electron density is found for the movement of another residue ARG 124 using step 1 of our method. The value for $q_{\max}$ is 0.22 Å^{-1} (crystallographic), corresponding to a resolution of about 5 Å, with maps calculated for a $50 \times 50 \times 50$ Å^3 box with an $11 \times 11 \times 11$ grid. This figure was produced with CHIMERA [16].

that give the best agreement with an experimental spectrum by finding the global minimum of the cost function. Although the global minimum of the cost function may involve temporarily increasing its value as a function of the parameters, this usually works due to the employment of a strategy based on the analogy with the physical process of annealing. Normally, simulated annealing would not be feasible for problems of this kind because varying the positions of all the atoms of the sample would not be feasible. Like the latter process it is a method generally capable of overcoming temporary barriers in order to find a global minimum. The main problem with simulated annealing is that the time taken by the process scales as a high power of the number of parameters, N^6. If N can be kept small, the method becomes feasible. Our strategy for keeping N small is finding the residue which is displaced in the rapid direct method described in the last section.

We use a cost function $[I_{\text{expt}} - I_{\text{the}}(R_j)]^2$ that is minimized by varying the coordinates of the atoms R_j. I_{the}, the model

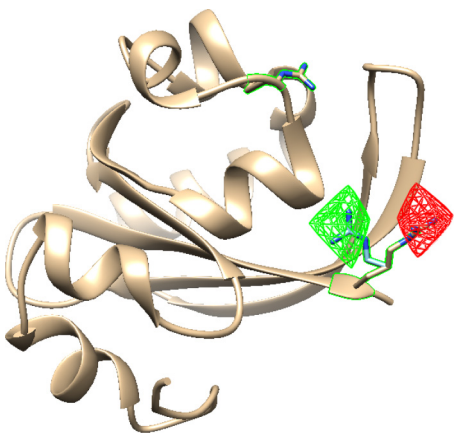

FIG. 6. Same as Fig. 8, except that the difference electron density is recovered from displacements of ARG 124 residue from classical time-resolved crystallography using the difference Fourier method.

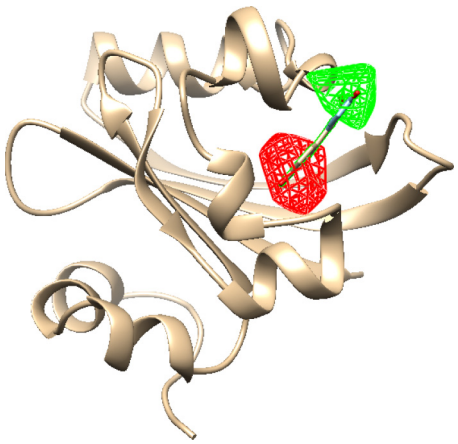

FIG. 7. Same as Fig. 3, but after step 2 of our algorithm. It can be seen that the small red and green lobes of Fig. 3 are now expanded out to be somewhat similar to Fig. 4 using the classical difference Fourier method of time-resolved crystallography.

intensities, thus vary as a function of the atom coordinates R_j. Since each atom can normally be described by three coordinates, the number of atoms can be related to the number of parameters by a maximum factor of 3 (the number of physical dimensions), although application of chemical constraints will reduce this considerably. If we assume the moved atoms lie within a residue containing these peaks of the direct method, the number N of parameters R_j can be kept fairly small, and the solution is feasible. The PYP molecule, for instance, contains about 1000 atoms, but a single residue contains about 10. Thus, assuming the time goes up as N^6 as Rous [15] indicates, this is automatically at least a trillionfold reduction in the time taken compared with the time to solve the entire molecule. The calculation currently runs for a few hours on an ordinary laptop. If Rous is right, trying to find the positions of all the atoms in the protein by simulated annealing on an ordinary laptop would take about a billion years! Consequently, simulated annealing

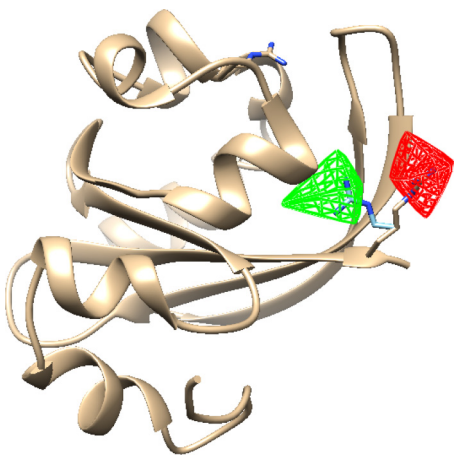

FIG. 8. Same as Fig. 5, except that the difference electron density is now recovered after step 2 of our algorithm. It can be seen that the small red and green lobes of Fig. 5 are now expanded out to be somewhat similar to Fig. 6 using the classical difference Fourier method of time-resolved crystallography.

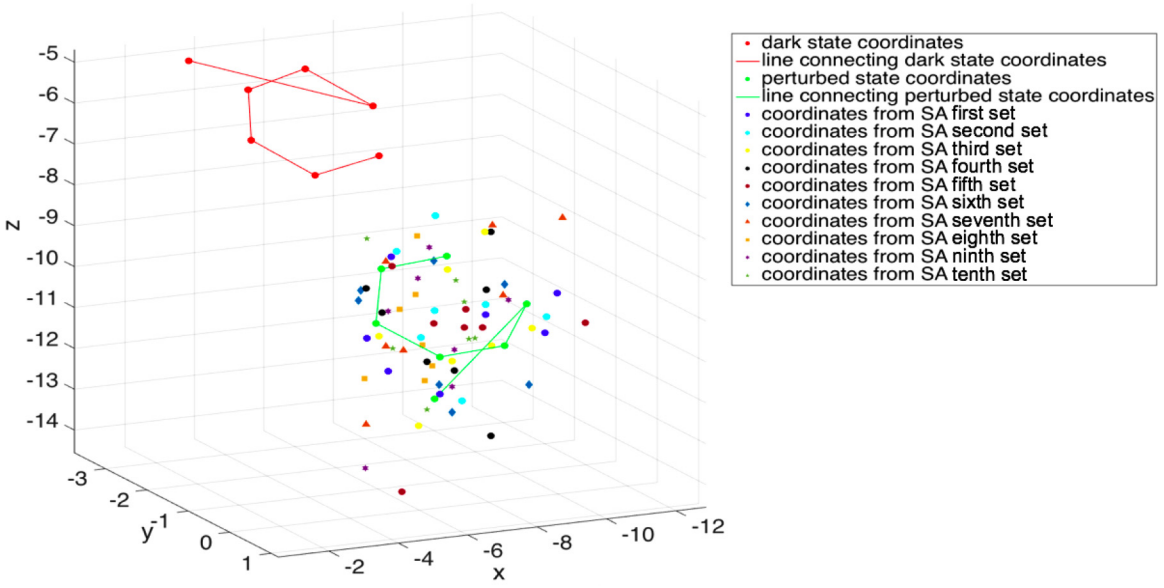

FIG. 9. Atomic coordinates of the chromophore in unperturbed and perturbed states and recovered by simulated annealing.

is not a method for finding a structure from scratch. Rather, if an approximate structure can be found by some means, it is excellent as a method of refinement, hence its use in this case in conjunction with a "direct" method of limited resolution.

VI. RESULTS OF SIMULATED ANNEALING

Although it is obvious from the difference electron density maps that the agreement after the simulated annealing is superior, we also plot the relevant atomic coordinates of the unperturbed structure (the starting point) and of the perturbed structure (the ultimate goal) as well as the coordinates as determined by simulated annealing. Ten different sets of coordinates are determined from simulated annealing. It will be seen that the simulated annealing finds the correct coordinates to within about 2 Å in the worst case. Figures 4, 6, 7, and 8 are produced with CHIMERA [16].

Figures 4 and 7 are concerned with the displacements of the chromophore (which is expected on photoexcitation), but Figs. 6 and 8 are concerned with the artificial displacement of a residue ARG 124 far from the chromophore in order to test our algorithm. In all cases we first used Eq. (15) to get an approximate electron density and then varied the positions of atoms within the residue by simulated annealing to obtain the exact atomic displacements. The efficacy of the simulated annealing algorithm may be judged by Fig 9. At least in the case where all the atomic displacements are found within the residues identified by the direct method our method seems to correctly identify the moved atoms, as verified by a comparison with the results from the tested difference Fourier method of time-resolved crystallography.

VII. CONCLUSIONS

Until now it has been necessary to crystallize proteins to find the time variation of such molecules. This is a limitation for two reasons. Not all proteins are easily crystallized. Indeed, there are a number of important membrane proteins that are very difficult to crystallize due to the presence of hydrophobic surfaces on their exteriors. Second, it is questionable whether the time-resolved structures found by conventional time-resolved crystallography are not artificial due to the presence of steric constraints from neighboring unit cells. We described here a two-step process that eventually gives a resolution for disordered molecules in SAXS/WAXS similar to that obtained in classical time-resolved crystallography on crystallized proteins. It is certainly arguable, therefore, that structures recovered from the solution are more representative of proteins under physiological conditions. We have successfully demonstrated the validity of our algorithm, but there are a number of assumptions and limitations. First, we assumed that the magnitudes of atomic displacements seen in time-resolved crystallography are also the same in the SAXS/WAXS experiment. Accordingly, we assumed that there is an average behavior in the solution that leads to a narrow distribution within each member of the pair of states. We also neglected in our artificial data the effect of the solvent, which may be a source of noise in difference spectra. We also assumed no noise in our demonstration. It is possible that the development of a reliable and reasonably fast method for SAXS/WAXS could be of crucial importance for the study of time-resolved structures under physiological conditions. For example, a recent experiment by Arnlund *et al.* [17] purports to explain the apparent promotion of chemical reactions that require only meV of energy, although the photon from the sun has, perhaps, an energy of about 1 eV. The postulation is the formation of a "protein quake" in the material to dissipate most of the energy. There is some evidence for this from molecular dynamics, although since this is a theoretical technique that depends on a number of assumptions, this evidence is not as strong as if structural evidence of a protein quake were obtained directly from SAXS/WAXS experiments alone. What has been lacking up to now is a method to recover the structure of

time-resolved changes directly from experiments. The method has performed well in our initial tests on simulated, artificial data. It remains to be seen how the theory here can be applied to experiment.

Of course, an assumption is that step 1 identifies the residues in which atoms move. Our ideas extend the previous work on extracting information from the difference in SAXS/WAXS spectra [18,19] by providing direct and objective locations of differences in the molecular structure. While this is true of time-resolved changes of PYP as a result of photoexcitation, it remains to be seen how general this is for a typical time-resolved structure.

ACKNOWLEDGMENTS

We acknowledge support for this work from a National Science Foundation Science and Technology Center (NSF Grant No. 1231306). We thank Dr. S. Wibowo for helpful discussions and the UWM High Performance Computing Center (HPC) for the use of the Avi cluster.

[1] H. B. Stuhrmann, New method for determination of surface form and internal structure of dissolved globular proteins from small angle x-ray measurements, Z. Phys. Chem. (Muenchen, Ger.) **72**, 177 (1970).

[2] H. B. Stuhrmann, Interpretation of small-angle scattering functions of dilute solutions and gases—A representation of structures related to a one-particle-scattering function, Acta Crystallogr. Sect. A **26**, 297 (1970).

[3] D. I. Svergun and H. B. Stuhrmann, New developments in direct shape determination from small-angle scattering. 1. Theory and model-calculations, Acta Crystallogr. Sect. A **47**, 736 (1991).

[4] K. Moffat, Time-resolved crystallography, Acta Crystallogr. Sect. A **54**, 833 (1998).

[5] K. Pande, C. D. M. Hutchison, G. Groenhof, A. Aquila, J. S. Robinson, J. Tenboer, S. Basu, S. Boutet, D. P. DePonte, M. N. Liang, T. A. White, N. A. Zatsepin, O. Yefanov, D. Morozov, D. Oberthuer, C. Gati, G. Subramanian, D. James, Y. Zhao, J. Koralek, J. Brayshaw, C. Kupitz, C. Conrad, S. Roy-Chowdhury, J. D. Coe, M. Metz, P. L. Xavier, T. D. Grant, J. E. Koglin, G. Ketawala, R. Fromme, V. Srajer, R. Henning, J. C. H. Spence, A. Ourmazd, P. Schwander, U. Weierstall, M. Frank, P. Fromme, A. Barty, H. N. Chapman, K. Moffat, J. J. van Thor, and M. Schmidt, Femtosecond structural dynamics drives the tran/cis isomerization in photoactive yellow protein, Science **352**, 725 (2016).

[6] M. Schmidt, Mix and inject: Reaction initiation by diffusion for time-resolved macromolecular crystallography, Adv. Condens. Matter Phys. **2013**, 167276 (2013).

[7] H. S. Cho, N. Dashdorj, F. Schotte, T. Graber, R. Henning, and P. Anfinrud, Protein structural dynamics in solution unveiled via 100-ps time-resolved x-ray scattering, Proc. Natl. Acad. Sci. USA **107**, 7281 (2010).

[8] H. M. Berman, J. Westbrook, Z. Feng, G. Gilliland, T. N. Bhat, H. Weissig, I. N. Shindyalov, and P. E. Bourne, The protein data bank, Nucleic Acids Res. **28**, 235 (2010).

[9] P. Hohenberg and W. Kohn, Inhomogeneous electron gas, Phys. Rev. **136**, B864 (1964).

[10] P. C. Hansen, The truncated SVD as a method for regularization, BIT Numer. Math. **27**, 534 (1987).

[11] T. W. Kim, J. H. Lee, J. Choi, K. W. Kim, L. J. van Wilderen, L. Guerin, Y. Kim, Y. O. Jung, C. Yang, J. Kim, M. Wulff, J. J. van Thor, and H. Ihee, Protein structural dynamics of photoactive yellow protein in solution revealed by pump-probe x-ray solution scattering, J. Am. Chem. Soc. **134**, 3145 (2012).

[12] G. E. O. Borgstahl, D. R. Williams, and E. D. Getzoff, 1.4 Å structure of photoactive yellow protein, a cytosolic photoreceptor: Unusual fold, active site, and chromophore, Biochemistry **34**, 6278 (1995).

[13] S. Kirkpatrick, C. D. Gelatt, and M. P. Vecchi, Optimization by simulated annealing, Science **220**, 671 (1983).

[14] H. C. Poon, M. Schmidt, and D. K. Saldin, Extraction of fast changes in the structure of a disordered ensemble of photoexcted biomolecules, Adv. Condens. Matter Phys. **2013**, 750371 (2013).

[15] P. J. Rous, A global approach to the search problem in surface crystallography by low energy electron diffraction, Surf. Sci. **296**, 358 (1993).

[16] E. F. Pettersen, T. D. Goddard, C. C. Huang, G. S. Couch, D. M. Greenblatt, E. C. Meng, and T. E. Ferrin, UCSF Chimera—A visualization system for exploratory research and analysis, J. Comput. Chem. **25**, 1605 (2004).

[17] D. Arnlund, L. C. Johansson, C. Wickstrand, A. Barty. G. J. Williams, E. Malmerberg, J. Davidsson, D. Milathianaki, D. P. De Ponte, R. L. Shoeman, D. Wang, D. James, G. Katona, S. Westenhoff, T. A. White, A. Aquila, S. Bari, P. Berntsen, M. Bogan, T. Berndt van Driel, R. B. Doak, K. S. Kjaer, M. Frank, R. Fromme, I. Grotjohann, R. Henning, M. S. Hunter, R. A. Kirian, I. Kosholeva, C. Kupitz, M. Liang, A. V. Martin, M. M. Nielson, M. Meeserschmidt, M. M. Siebert, J. Sjohann, F. Stellato, U. Weierstall, N. A. Zatsepin, J. C. H. Spence, P. Fromme, I. Schlichting, S. Boutet, G. Groenhof, H. N. Chapman, and R. Neutze, Visualizing a protein quake with time-resolved X-ray scattering at a free electron laser, Nat. Methods **11**, 923 (2014).

[18] S. Ahn, K. H. Kim, Y. Kim, J. Kim, and H. Ihee, Protein tertiary structural changes visualized by time-resolved x-ray solution scattering, J. Phys. Chem. B **113**, 13131 (2009).

[19] E. Malmberg, Z. Omran, J. S. Hub, X. W. Li, G. Kantona, S. Westenhoff, L. C. Johansson, M. Andersson, M. Cammarata, M. Wulff, D. van der Spoel, J. Davidsson, A. Specht, and R. Neutze, Time-resolved WAXS reveals accelerated conformational changes in iodoretinal-substituted proteorhodopsin, Biophys. J. **101**, 1345 (2011).